Seeing through biological tissues using the fly eye principle

Joseph Rosen and David Abookasis

Ben-Gurion University of the Negev
Department of Electrical and Computer Engineering
P. O. Box 653, Beer-Sheva 84105, Israel
dudua@ee.bgu.ac.il , rosen@ee.bgu.ac.il

Abstract: During the past decade, optical imaging through scattering medium has proved to be a powerful technique for many applications. It is especially effective in medical diagnostic, since it is safe, noninvasive and low-cost compared with the conventional radiation techniques. Based on a similar principle of the fly's visual system, we show a novel method of optical imaging through scattering medium. An image of bones hidden between two biological tissues (chicken breast) is recovered from many noisy speckle pictures obtained on the output of a multi-channeled optical imaging system. The operation of multiple imaging is achieved using a microlens array. Each lens from the array projects a different speckled image on a digital camera. The set of speckled images from the entire array are first shifted to a common center and then accumulated to a single average picture in which the concealed object is exposed.

OCIS codes: (170.3880) Medical and biological imaging; (110.6150) Speckle imaging

References

1. R. Dawkins, *Climbing Mount Improbable* (W. W. Norton & Co., 1996), 138-197.
2. M. F. Land, and D.-E. Nilsson, *Animal Eyes* (Oxford Univ. Press, New York, 2002), 125-155.
3. J. C. Hebden, S. R. Arridge and D. T. Delpy, "Optical imaging in medicine: I. Experimental techniques," Phys. Med. Biol. **42**, 825-840 (1997).
4. J. W. Goodman, *Introduction to Fourier Optics*, 2nd ed. (McGraw-Hill, New York, 1996), 126-130.
5. T. Vo-Dinh *ed*., Biomedical Photonics Handbook (CRC Press, Boca Raton 2003), **21**-8.
6. L. Wang, and S. L. Jacques, "Use of a laser beam with an oblique angle of incidence to measure the reduced scattering coefficient of a turbid medium," Appl. Opt. **34**, 2362-2366 (1995).
7. W.-F. Cheong, S. A. Prahl, and A. J. Welch, "A review of the optical properties of biological tissues," IEEE J. Quantum Electron. **26**, 2166-2185 (1990).
8. H. Arimoto, and B. Javidi, "Integral three-dimensional imaging with digital reconstruction," Opt. Lett. **26**, 157-159 (2001).

The compound eye is the most common eye in the nature [1], but species of the fly have special kind of compound eyes equipped with visual system called neural superposition. Neural superposition means that several (seven according to Ref. [2]) identical images from several facets are superposed together to a single common image by neural connections of the photoreceptors. Land and Nilsson [2] explain that the advantage of the neural superposition is in the gain of the observed image which enables the flies to see better than their competitors under faint illumination conditions. The question whether it is the only advantage is still open, but the problem we consider here is whether any engineering visual system following the principle of neural superposition might have any useful purpose. Obviously, the nowadays digital cameras have more efficient ways to gain a single recorded image without capturing multiple images of the same scene. This study shows that by using the fly eye principle, i.e.,

#3320 - $15.00 US Received November 07, 2003; Revised December 18, 2003

superposing multiple images from many imaging channels, enables one to see general objects hidden behind scattering layers. In recent years much effort has been devoted to research in the optical imaging of objects embedded in a scattering medium, and different optical imaging techniques have been proposed [3]. This topic has many potential applications in medical diagnostics since it is safe, noninvasive, and relatively inexpensive compared with other often-used tomography techniques.

In this work we propose a new scheme of seeing through scattering medium which is similar to the fly's visual system. This system averages over an ensemble of noisy speckle images and therefore we term the system as Noninvasive Optical Imaging by Speckle Ensemble (NOISE). In order to collect different blurred images of the same object, the object should be observed from unrelated spatial parts of the same scattering medium. This goal is achieved by use of microlens array (MLA), where each lens from the array images the same object through different part of the scattering layer. In the experimental system, shown in Fig. 1, the object hidden between two scattering tissues is coherently illuminated from its back by a plane wave. Each lens of the array, together with the spherical lens L, operate as two successive imaging systems. Without the scattering layers, the illuminated coherently system is characterized by a relatively narrow point spread function (PSF) [4] $h_o(x,y)$. This PSF is calculated conventionally as an inverse Fourier transform of the aperture of a single micro-lens. In the present case, the micro-lens imposes the system bandwidth because its numerical aperture is smaller than that of the lens L.

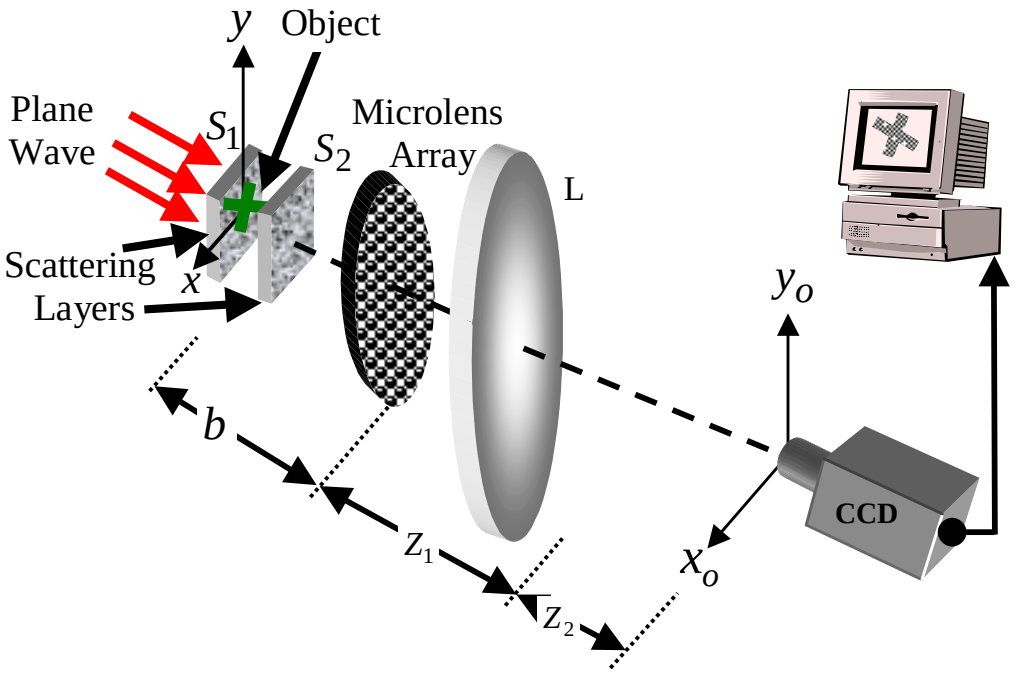

Fig. 1. Setup of the NOISE system.

Next, we consider the effect of the back scattering layer S_1. This layer diffuses the light such that each micro-lens gets almost uniformly part of the illumination. In addition, because of the randomness of the medium S_1 and its uniformity, the object is multiplied by a random phase function with almost constant magnitude. The entire system is modeled as an array of several identical imaging systems, all with the same PSF given by $h_o(\boldsymbol{r})$, where $\boldsymbol{r}=(x,y)$ is the

#3320 - $15.00 US Received November 07, 2003; Revised December 18, 2003

position vector. In each imaging channel the input function is $t(\boldsymbol{r})=A(\boldsymbol{r})\exp[i\phi(\boldsymbol{r})]$, where $A(\boldsymbol{r})$ stands for the object amplitude function and $\phi(\boldsymbol{r})$ is a random phase function induced by layer S_1. The image intensity at the k-th coherently illuminated channel is given by[4]

$$I(\boldsymbol{r}_o) = |t(\boldsymbol{r}_o) * h_o(\boldsymbol{r}_o)|^2 \tag{1}$$

where asterisk denotes two-dimensional convolution, and $\boldsymbol{r}_o=(x_o,y_o)$ is the position vector on the output plane. $I(\boldsymbol{r}_o)$ of Eq. (1) is the diffraction limited image of the squared function of the object, $|A(\boldsymbol{r}_o)|^2$. The goal of the following proposed process is to produce intensity distribution as close as possible to $I(\boldsymbol{r}_o)$.

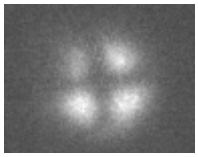

Fig. 2. The average picture of the entire array when the cross-junction of chicken bones is positioned in front of layer S_1 and the layer S_2 is removed

When the front scattering layer S_2 is introduced into the system, the output image is distorted such that the object cannot be recognized. Since each micro-lens observes the object through a different transverse cross-section of the scattering layer, each k-th micro-lens together with the lens L create a linear system characterized by a different random PSF $h_k(\boldsymbol{r})$. Therefore, the output intensity pattern in each coherently illuminated k-th channel is given by $\tilde{I}_k(\boldsymbol{r_o}) = |t(\boldsymbol{r_o}) * h_k(\boldsymbol{r_o})|^2$. It is assumed that although each PSF $h_k(\boldsymbol{r})$ is a random function, wider than $h_o(\boldsymbol{r})$, the ensemble average PSF over the entire K channels satisfies the relation:

$$\frac{1}{K}\sum_k h_k(\boldsymbol{r}) \cong h_o(\mathrm{r}). \tag{2}$$

This assumption is valid for scattering mediums satisfying statistics of Rytov model with weak phase modulation and Born model [5]. Having the set of K speckled images $\{\tilde{I}_k(\boldsymbol{r}_o)\}$, we first center each one of them and then sum them to a single average image given by,

$$S(\boldsymbol{r_o}) = \frac{1}{K}\sum_k |t(\boldsymbol{r_o}) * h_k(\boldsymbol{r_o})|^2 \tag{3}$$

Based on Eq. (2), it can be shown that the average image is approximately,

$$S(\boldsymbol{r_o}) \cong |t(\boldsymbol{r_o}) * h_o(\boldsymbol{r_o})|^2 + |t(\boldsymbol{r_o})|^2 * \sigma^2(\boldsymbol{r_o}) \tag{4}$$

where σ^2 is the variance of the random set $\{h_k(\boldsymbol{r})\}$, defined as $\sigma^2(\boldsymbol{r}) = 1/K \sum_k |h_k(\boldsymbol{r}) - h_o(\boldsymbol{r})|^2$ The first term of Eq. (4) is approximately the desired diffraction-limited image given by Eq. (1). The second term is a convolution between the object and the variance functions. Clearly $\sigma^2(\boldsymbol{r})$ is wider than $h_o(\boldsymbol{r})$ because the scattering layer broaden the diffraction-limited image of a point. Therefore, we conclude that the second convolution in Eq. (4) blurs the diffraction-limited image of the object. The value of this blurring term is determined by the average value of the variance $\sigma^2(\boldsymbol{r})$. The contrast and the sharpness of the reconstructed object are inversely dependent on the variance.

To demonstrate the proposed technique, an opaque object made of chicken bones in a shape of a cross-junction with the size of $9\times9mm$ was embedded between two layers of

#3320 - $15.00 US Received November 07, 2003; Revised December 18, 2003

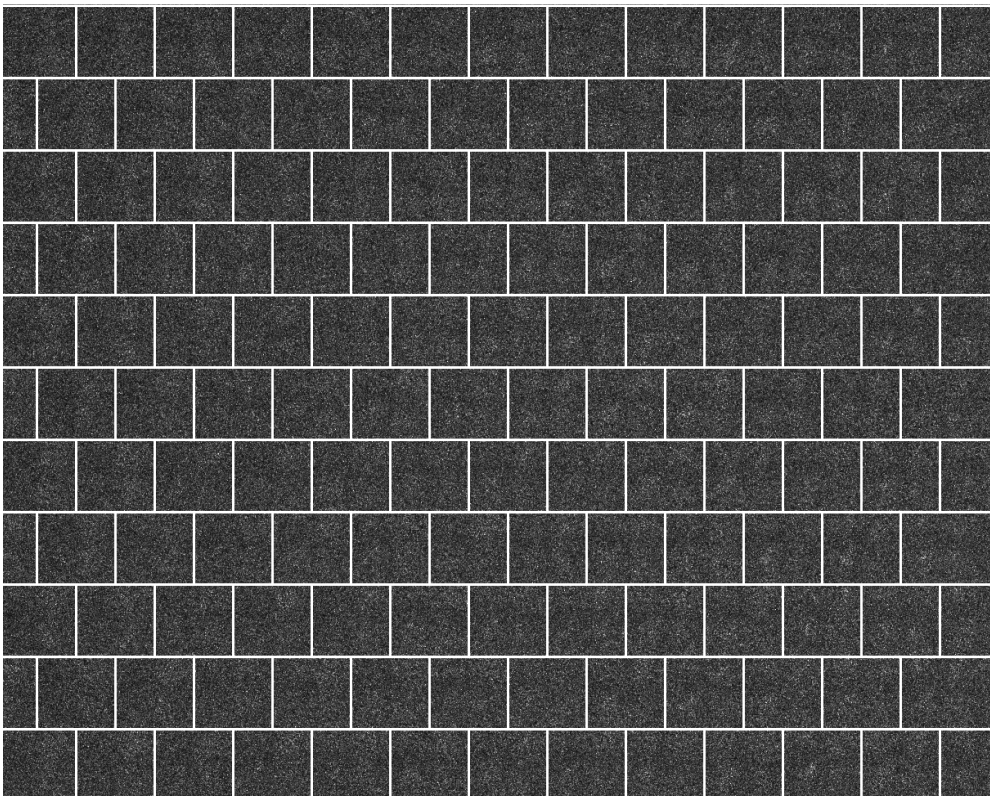

Fig. 3. 12×11 blurred images recorded by the CCD when the cross-junction sign is embedded between the two scattering layers.

chicken breast separated from each other by a distance of 12*mm*. Fig. 2 shows the average picture of the exposed cross-junction of bones over the entire array when only layer S_1 exists in the set up, and S_2 is removed. The thickness of the rear tissue S_1 was about 3*mm*, whereas the thickness of the front tissue S_2, was about 8*mm*. The reduced scattering coefficient of the tissues of μ_s'=4.5±0.3cm^{-1} was measured by the method proposed in Ref. [6]. Assuming the anisotropy factor[7] is g=0.965, The scattering coefficient becomes $\mu_s = \mu_s^{'}/(1-g) = 128 \pm 9 cm^{-1}$. The rear tissue S_1 was illuminated by a collimated plane wave of 35*m*W He-Ne laser with λ=632.8*nm* wavelength. The MLA, placed a distance of b=160*mm* from the object, was composed of 115×100 hexagonal refractive lenses. A similar MLA has been used in integral imaging systems for purpose of three-dimensional imaging [8]. Only the central 132=12×11 lenses were used in the present experiments. The radius of each micro-lens was r_l=250μm and its focal length was 3.3*mm*. Under these conditions the optical system without the tissues can resolve a minimum size of $\lambda b/r_l \cong 0.4mm$. The resolution can be improved using lenses with larger apertures. However, this change may increase the total view angle of the system and thus the various channels may image different perspectives with different shapes of the same object. The image plane of the MLA was projected onto the CCD plane by a single spherical lens L, with a 300*mm* focal length. The distance Z_1 and Z_2 shown in Fig. 1 were 520*mm* and 710*mm*, respectively. In the experiment we used a CCD camera with 1280(H)×1024(V) pixels, within 8.6×6.9*mm* square active area.

Figure 3 shows the array of all speckled images recorded by the CCD, whereas the embedded object was the cross-junction of bones. The white lines indicate the image area

#3320 - $15.00 US Received November 07, 2003; Revised December 18, 2003

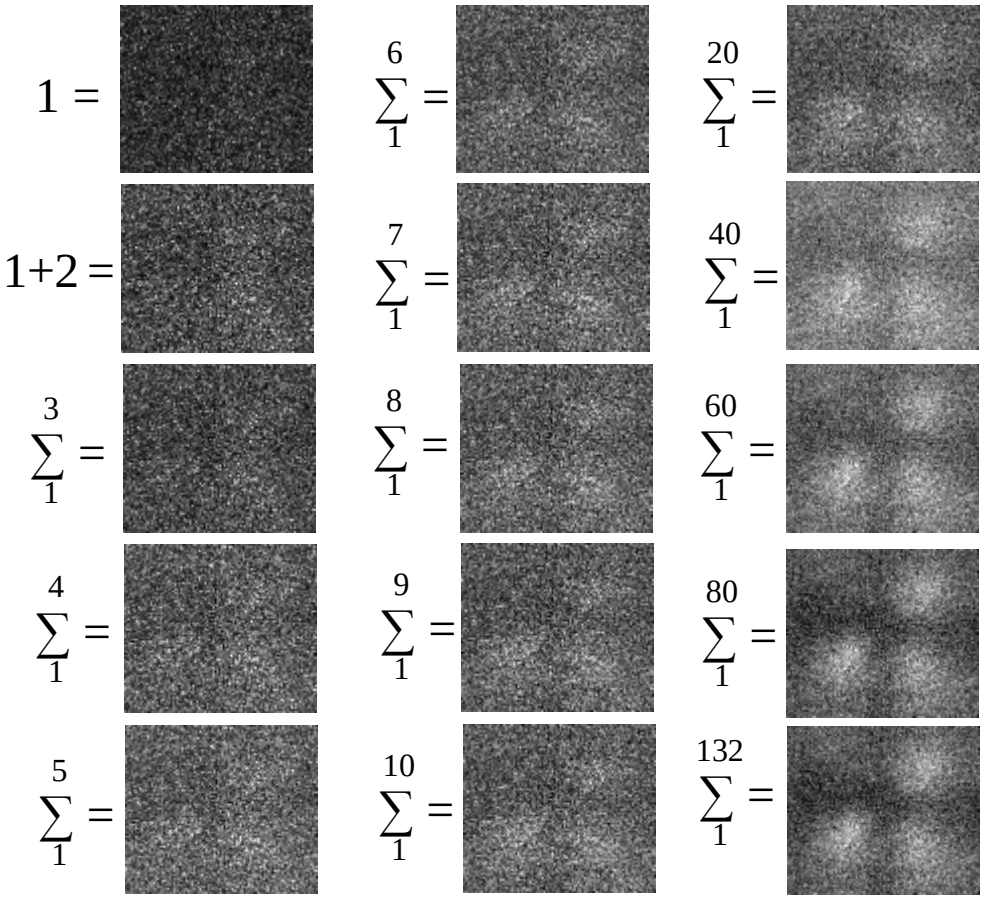

Fig. 4. The process of recovering the hidden object by adding more and more pictures from the array of 132 pictures shown in Fig. 3.

contributed by each single lens. These lines were synthetically added on the original captured picture only for clarity. The original object cannot be recognized from any image of the 132 different blurred images shown in Fig. 3. An enlarged example from the set of Fig. 3 is presented in the upper left corner of Fig. 4. Each blurred sub-image of the size 96×84 pixels from the array was extracted from the matrix, and was shifted toward a common center. We calculated the center of gravity of each contrast-inverted blurred cloud of the entire set of 132 blurred images. The center of gravity is considered as the true center of the object in each frame, and accordingly all the images are centered to have the same center of gravity. We assume that the angular difference between the most extreme view points is small enough (less than 3^{o} in the present experiment) to neglect the differences between all the various perspectives of the object observed from the various channels. Although the lateral shift of the object image depends on the longitudinal position of the object in the scattering layers (denoted as *b* in Fig. 1), it does not mean that one should know the longitudinal position of the object in the scattering layers in prior to image the object. The algorithm of calculating the blurred image's center of gravity yields the various positions of the object in all the channels regardless of object's longitudinal position. The reconstruction process is shown in Fig. 4. Each image is a sum of different amount of images from 1 to 132 in horizontal scanning order from the most left picture in the array of Fig. 3. Naturally, as more images are summed together, the cross-junction of bones becomes clearer. Also, note that the most dramatic

#3320 - $15.00 US Received November 07, 2003; Revised December 18, 2003

improvements in the image happen during the summation of the first 10 pictures, and adding more pictures beyond 70 do not improve much the final image. These observations are quantitatively demonstrated by the plot of the average mean square error (MSE) between the final image, averaged over 132 images, and every partial summation from 1 to 132 (the blue line of Fig. 5). Indeed the improvement after the first 65 pictures is relatively small. The red line of Fig. 5 shows the MSE between the non-scattered object of Fig. 2 and the images obtained from *N* additions. This plot indicates that after 85 additions the MSE reduction is negligible. These results indicate that we could reduce the number of channels by about half and gain more resolution, or alternatively we could hide the object behind a thicker scattering layer and still distinguish the object.

To verify that it is necessary to use coherent light, we imaged through the same scattering layers with incoherent light. The picture obtained in each channel is a wide blurry spot. All the pictures of the set seem to be more or less the same wide smoothly blurry spots. Averaging over all 132 pictures yields again a wide smoothly blurry spot. Incoherent light means that the object is illuminated by a large number of plane waves with many different angles. The effect on the output image in each channel is an accumulation of many blurred images of the object shifted randomly from the true object center. Therefore the result in each imaging channel is a smoothly blurred unrecognizable image of the object. Accumulating these images along all the channels does not allow us to see through the scattering medium.

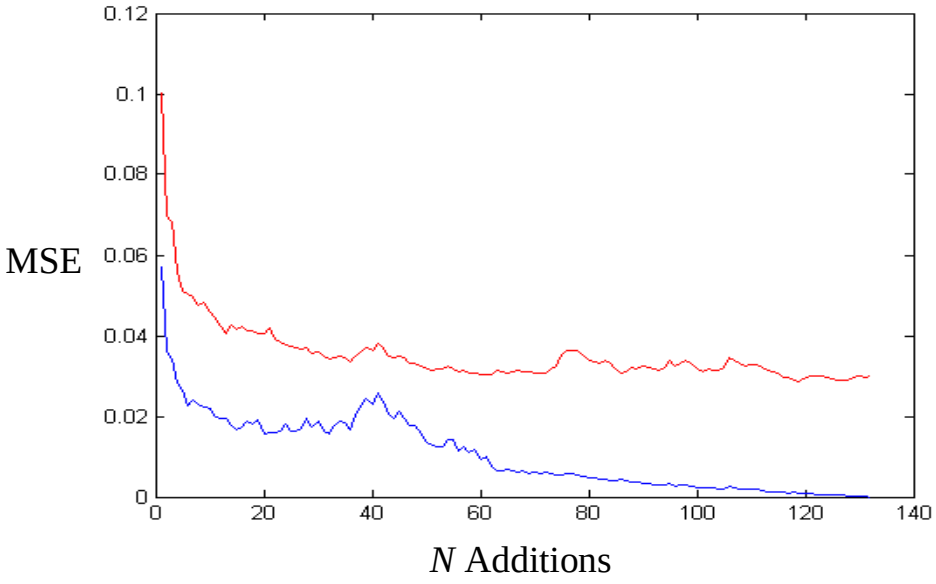

Fig. 5. Average Mean Square Error versus the number of additions, where *N* goes from 1 to 132. Blue line – MSE between the final image and the images obtained from *N* additions. Red line – MSE between the images of Fig. 2 and the image obtained from *N* additions.

In conclusion, by the NOISE technique we have been able to reconstruct the shape of objects embedded between two scattering layers. The weakness of the present setup is the relatively low spatial bandwidth product of the diffraction limited system. The use of a small aperture lens at each imaging channel reduces both the field of view and the system's bandwidth. However, this drawback seems as a reasonable penalty to pay for the ability to see through scattering medium in a simple and robust way. The advantages of the method are relative simplicity, low cost, fast operation and the need of low power CW laser illumination. Because of all these advantages NOISE might be useful for many imaging applications, especially in the medical diagnostic.

#3320 - $15.00 US Received November 07, 2003; Revised December 18, 2003

Acknowledgments

This research was supported by the Israel Science Foundation grant 119/03.

#3320 - $15.00 US Received November 07, 2003; Revised December 18, 2003